

Latent Network Structure Learning from High Dimensional Multivariate Point Processes

Biao Cai, Jingfei Zhang and Yongtao Guan

*Department of Management Science, Miami Herbert Business School,
University of Miami, Coral Gables, FL, 33146.*

Abstract

Learning the latent network structure from large scale multivariate point process data is an important task in a wide range of scientific and business applications. For instance, we might wish to estimate the neuronal functional connectivity network based on spiking times recorded from a collection of neurons. To characterize the complex processes underlying the observed data, we propose a new and flexible class of non-stationary Hawkes processes that allow both excitatory and inhibitory effects. We estimate the latent network structure using an efficient sparse least squares estimation approach. Using a thinning representation, we establish concentration inequalities for the first and second order statistics of the proposed Hawkes process. Such theoretical results enable us to establish the non-asymptotic error bound and the selection consistency of the estimated parameters. Furthermore, we describe a penalized least squares based statistic for testing if the background intensity is constant in time. We demonstrate the efficacy of our proposed method through simulation studies and an application to a neuron spike train data set.

Keywords: Hawkes process; non-asymptotic error bound; nonlinear; nonstationarity; selection consistency.

1 Introduction

Large-scale multivariate point process data are fast emerging in a wide range of scientific and business applications. Learning the latent network structure from such data has become an increasingly important task. For instance, one may wish to estimate the neuronal functional connectivity network based on spiking times (i.e., times when a neuron fires) recorded from a collection of neurons (Farajtabar et al., 2015), or to estimate the financial network based on trading times recorded for a collection of stocks (Linderman and Adams, 2014). Both the neuron spiking times and the trading times can be viewed as realizations from multivariate point processes. To characterize the latent interactions between the different point processes, a useful class of models is the multivariate Hawkes process (Hawkes, 1971). The multivariate Hawkes process is a mutually-exciting point process, in which the arrival of one event in one point process may trigger those of future events across the different processes. Because of its flexibility and interpretability, the multivariate Hawkes process has been widely used in many applications, such as social studies (Zhou et al., 2013), criminology (Linderman and Adams, 2014), finance (Bacry et al., 2013) and neuroscience (Okatan et al., 2005). In the network setting, each component point process of the multivariate Hawkes process is viewed as a node. A directed edge connecting two nodes indicates an event in the source point process increases the probability of occurrence of future events in the target point process. Recently, work such as Xu et al. (2016) connected such networks to the notion of Granger causality.

Despite the popularity of the multivariate Hawkes process, there is a need of new statistical theory and methodology for its broader applications. *First*, most existing theoretical results for the Hawkes process are derived using a cluster process representation of the process. This cluster process representation by its definition depends on the mutually excitation assumption, that is, the arrival of one event increases the probability of occurrence of future events (Hawkes and Oakes, 1974; Hansen et al., 2015). However, such an assumption may not be valid in certain applications. For example, it is well known that the firing activity of one neuron can inhibit the activities of other neurons (Amari, 1977). A more flexible model should allow both excitatory and inhibitory effects, which renders the cluster process representation infeasible. *Second*, most existing models assume that the background intensities, i.e., the baseline arrival rates of events from the different component processes, are constant in time. Under this assumption, the multivariate Hawkes process satisfies a stationary condition (e.g., Brémaud and Massoulié, 1996). However, assuming constant background

intensities may also be too restrictive in practice. For example, stock trading activities tend to be much higher during market opens and closes (Engle and Russell, 1998), and the associated background intensities are therefore not constant in time. A multivariate Hawkes process with constant background intensities may not fit such data well (Chen and Hall, 2013). A more flexible approach instead should allow the background intensities to be time-varying. For such nonstationary models, new development on both theory and methodology is needed, as most existing results are established assuming the underlying process to be stationary.

Some existing work have considered broadening the class of Hawkes process models. Specifically, Brémaud and Massoulié (1996); Costa et al. (2018) considered a class of nonlinear Hawkes processes that allows both excitatory and inhibitory effects. A thinning process representation was used to investigate the properties of the proposed process. However, both work focused on processes with constant background intensities and the thinning representation technique depended critically on the stationarity condition. Chen et al. (2017) considered a similar class of models but restricted to the linear case. They derived the concentration inequality for the second order statistics of the process, and subsequently considered the latent network structure estimation. Similar to the above contributions, the proposed method and derived results also required the stationarity condition. Some recent work also considered nonstationary Hawkes processes. Lewis and Mohler (2011); Chen and Hall (2013); Roueff et al. (2016) considered Hawkes processes with time varying background intensities. However, they only considered univariate processes, and only with excitatory effects. Lemonnier and Vayatis (2014) considered a multivariate Hawkes process with time varying background intensities. However, they focused on an approximate optimization algorithm for model estimation, and did not provide any theoretical results.

In this article, we propose a flexible class of multivariate Hawkes process that admits time-varying background intensities and allows both excitatory and inhibitory effects. We show the existence of a thinning process representation of this nonstationary process. Such a result has not yet been established in the literature, and it enables our subsequent theoretical analysis of the network structure estimation. Next, to estimate the network structure, we consider a computationally efficient penalized least squares estimation, in which both the background intensities and the transfer functions are approximated using basis functions. We establish theoretical properties of the penalized least squares estimator in the high-dimensional regime, where the dimension of the multivariate process grows faster than the

length of the observation window. Specifically, we investigate the following properties in our analysis:

1. (Concentration inequalities.) We establish concentration inequalities for the first and second order statistics of the proposed Hawkes process. Such inequalities are established using a thinning process representation and a coupling construction. The derived inequalities are subsequently used as important tools in investigating the theoretical properties of the penalized least squares estimator.
2. (Non-asymptotic error bound.) Under certain regulatory conditions, we establish, in the high-dimensional regime, the non-asymptotic error bound of the intensity functions estimated using the penalized least squares approach.
3. (Network recovery.) We show that, under certain regulatory conditions, our proposed estimation method can consistently identify the true edges in the network with probability tending to one. This result is established under a much relaxed condition when compared to [Chen et al. \(2017\)](#), which considered a linear and stationary setting.
4. (Test for background intensity.) We propose a penalized least squares based statistic for testing if the background intensity is constant in time. Specially, we show that the test statistic follows a mixture of χ^2 distributions asymptotically.

We remark that there is another class of approaches that estimate the latent network structure from high dimensional multivariate point process data ([Zhang et al., 2016](#); [Vinci et al., 2016, 2018](#)). These methods divide the observation window into a number of bins, and model the number of events in each bin. The network structure is inferred using methods such as correlation of event counts ([Vinci et al., 2016](#)), regularized generalized linear models ([Zhang et al., 2016](#)), or Gaussian graphical models ([Vinci et al., 2018](#)). Such a type of approaches do not involve estimating the multivariate intensity function underlying the observed point patterns, and are potentially more computationally efficient. However, the ad hoc binning procedure may lose important information. For example, short-term excitatory effects may be overlooked if the bins are chosen to be too wide. It still remains unclear on how to choose a binning procedure, and what its effect is on the subsequent model estimation and analysis.

The rest of the article is organized as follows. Section 2 introduces the proposed model, and Section 3 describes the model estimation and selection. The aforementioned theoretical

results are detailed in Sections 4. Section 5 includes simulation studies. The detailed analysis of a neuron spike train dataset is presented in Section 6. All proofs are collected in the Supplementary Materials.

2 Model

Consider a directed network with p nodes. For each node $j \in \{1, 2, \dots, p\}$, we observe its event locations $\{t_{j,1}, t_{j,2}, \dots\}$ in the time interval $(0, T]$ such that $0 < t_{j,1} < t_{j,2} < \dots \leq T$. For node j , let the associated counting process be $N_j(t) = \max\{i : t_{j,i} \leq t\}$, $t \in (0, T]$. Write $\mathbf{N} = (N_j)_{j=1, \dots, p}$ as the p -variate counting process. Let \mathcal{H}_t denote the entire history of \mathbf{N} up to time t , and write $N_j([t, t + dt))$ as $dN_j(t)$. The p -variate intensity function $\boldsymbol{\lambda}(t) = (\lambda_1(t), \dots, \lambda_p(t))^\top$ of \mathbf{N} is defined as

$$\lambda_j(t)dt = \mathbb{P}(dN_j(t) = 1 | \mathcal{H}_t), \quad j = 1, \dots, p.$$

We propose a flexible class of Hawkes processes with intensity functions defined as

$$\lambda_j(t) = h \left\{ \nu_j(t) + \sum_{k=1}^p \int_0^t \omega_{j,k}(t-u) dN_k(u) \right\}, \quad j = 1, \dots, p, \quad (1)$$

where $\nu_j(\cdot) : \mathbb{R}^+ \rightarrow \mathbb{R}^+$ is the time-varying background (or baseline) intensity function of the j th process, and $\omega_{j,k}(\cdot) : \mathbb{R}^+ \rightarrow \mathbb{R}$ is the transfer function that characterizes the effect of the k th process on the j th process. The function $h(\cdot)$ is a θ -Lipschitz link function and $\theta \leq 1$. The Lipschitz condition on the link function has also been considered in establishing the stability of nonlinear Hawkes processes (Brémaud and Massoulié, 1996). Due to this condition, link functions such as $h(x) = \exp(x)$ cannot be considered in our model, as it is not θ -Lipschitz. Compared with existing Hawkes processes, our model in (1) allows the background intensity functions to be time-varying. Moreover, the transfer functions, i.e., $\omega_{j,k}$'s in (1), are not required to be nonnegative functions. As a result, both excitatory and inhibitory effects are allowed. Specifically, we have

- i. $\omega_{j,k}(s) > 0$ corresponds to *excitatory* effect, that is, an event in process k increases the probability of event occurrence in process j at a time distance of s .
- ii. $\omega_{j,k}(s) < 0$ corresponds to *inhibitory* effect, that is, an event in process k decreases the probability of event occurrence in process j at a time distance of s .

- iii. $\omega_{j,k}(s) = 0$ corresponds to no effect, that is, an event in process k has no effect on the event occurrence in process j at a time distance of s .

To ensure that the intensity function is nonnegative under this more flexible scenario, we apply the nonlinear link function $h(x) = \max(0, x)$. It is seen that this h is a non-decreasing θ -Lipschitz function, and $\theta \leq 1$.

Let the directed network $\mathcal{G}(\mathcal{V}, \mathcal{E})$ summarize the relationships between the p component processes. Specifically, let $\mathcal{V} = \{1, 2, \dots, p\}$ be the set of p nodes and \mathcal{E} be the set of edges such that

$$\mathcal{E} = \{(j, k) : \omega_{j,k} \neq 0, 1 \leq j, k \leq p\},$$

where $\omega_{j,k}$'s are the transfer functions in (1). Therefore, $(j, k) \in \mathcal{E}$ if and only if the k th process has an excitatory or inhibitory effect on the j th process. Recently, work such as [Xu et al. \(2016\)](#) connected such networks to the notion of Granger causality.

Next, we introduce a regularity condition on the background intensities and transfer functions in (1).

Assumption 1. *Let Ω be a $p \times p$ matrix with $\Omega_{jk} = \int_0^\infty |\omega_{j,k}(t)| dt$, $1 \leq j, k \leq p$. Assume that $\sigma_{\max}(\Omega^\top \Omega) \leq \sigma_\Omega < 1$, where $\sigma_{\max}(\Omega^\top \Omega)$ is the largest eigenvalue of the matrix $\Omega^\top \Omega$. Moreover, assume that the background intensity functions are bounded above by a constant ν , i.e., $\nu_j(t) \leq \nu$, $j = 1, \dots, p$.*

Under Assumption 1, the process in (1) has bounded mean intensity. To see this, we first have that, with some straightforward algebra, the mean intensity of (1) is upper bounded by the mean intensity of the Hawkes process $\mathbf{N}^* = (N_j^*)_{j=1, \dots, p}$ with intensity function

$$\lambda_j^*(t) = \nu + \sum_{k=1}^p \int_{-\infty}^t |\omega_{j,k}(t-u)| dN_k^*(u), \quad j = 1, \dots, p. \quad (2)$$

Define the mean intensity of (2) as $\mathbf{\Lambda}^* = (\Lambda_1^*, \dots, \Lambda_p^*)^\top \in \mathbb{R}^p$, where $\Lambda_j^* = \mathbb{E}\{dN_j^*(t)\}/dt$.

We have

$$\mathbf{\Lambda}^* = \boldsymbol{\nu} + \left\{ \int_0^\infty |\boldsymbol{\omega}(t)| dt \right\} \mathbf{\Lambda}^*, \quad (3)$$

where $\boldsymbol{\nu} = (\nu, \dots, \nu)^\top \in \mathbb{R}^p$ and $\boldsymbol{\omega}(t) \in \mathbb{R}^{p \times p}$, with $\boldsymbol{\omega}(t)_{jk} = \omega_{j,k}(t)$. With Assumption 1, we can rewrite (3) as $\mathbf{\Lambda}^* = \sum_{k=0}^\infty \boldsymbol{\Omega}^k \boldsymbol{\nu}$, which is bounded under Assumption 1. We note that the bounded eigenvalue condition in Assumption 1 is commonly considered in establishing the stability of multivariate Hawkes processes ([Brémaud and Massoulié, 1996](#)).

3 Estimation

From the observed event locations in $(0, T]$, our objective is to estimate the intensity functions $\lambda_j(t)$, $j = 1, \dots, p$. Furthermore, by identifying the non-zero transfer functions $\omega_{j,k}$'s in the estimated intensity functions, we can infer about the directed network $\mathcal{G}(\mathcal{V}, \mathcal{E})$. To ease notation, we write

$$\psi_j(t) = \nu_j(t) + \sum_{k=1}^p \int_0^t \omega_{j,k}(t-u) dN_k(u), \quad (4)$$

and $\lambda_j(t) = \max\{0, \psi_j(t)\}$, $j = 1, \dots, p$.

To estimate the intensity functions, one might consider a likelihood function based approach (Ogata, 1981; Chen and Hall, 2013; Zhou et al., 2013). However, the surface of the negative loglikelihood function of the Hawkes processes can be complex, especially when p is large, and highly nonconvex (Wang et al., 2016). Moreover, minimizing the negative loglikelihood function requires a very involved and computationally intensive iterative procedure (Veen and Schoenberg, 2008). To overcome the challenge of nonconvexity and improve the estimation efficiency, we alternatively consider a least squares loss based estimation approach. That is, we consider the following loss function

$$\frac{1}{T} \sum_{j=1}^p \int_0^T \{\psi_j^2(t) dt - 2\psi_j(t) dN_j(t)\}. \quad (5)$$

The least squares loss has been fairly commonly considered in estimating point process models (Bacry et al., 2015; Hansen et al., 2015; Chen et al., 2017). In our estimation approach, we show that (5) can be separated into p simple convex objective functions that can be estimated individually. This significantly reduces the computation cost of our estimation procedure. We remark that although the least squares loss is convex and reduces the computational cost, the obtained estimator is not as efficient as the maximum likelihood estimator. In Section 4, we investigate theoretical properties of the minimizer of (5).

Next, we approximate the background intensity $\nu_j(t)$ with an m_0 -dimensional basis $\boldsymbol{\phi}_0(t) = (\phi_{0,1}(t), \dots, \phi_{0,m_0}(t))$, such that $\nu_j(t) = \boldsymbol{\phi}_0(t) \cdot \boldsymbol{\beta}_{j,0} + r_{0,j}(t)$, where $r_{0,j}(\cdot)$ denotes the approximation residual and $\boldsymbol{\beta}_{j,0} \in \mathbb{R}^{m_0}$. Furthermore, we approximate the transfer functions $\omega_{j,k}(t)$ with an m_1 -dimensional basis $\boldsymbol{\phi}_1(t) = (\phi_{1,1}(t), \dots, \phi_{1,m_1}(t))$, such that $\omega_{j,k}(t) = \boldsymbol{\phi}_1(t) \cdot \boldsymbol{\beta}_{j,k} + r_{j,k}(t)$, where $r_{j,k}(\cdot)$ denotes the approximation residual and $\boldsymbol{\beta}_{j,k} \in \mathbb{R}^{m_1}$. The bases $\boldsymbol{\phi}_0(t)$ and $\boldsymbol{\phi}_1(t)$ are allowed to be different for more flexibility in characterizing the background intensities and transfer functions. For example, one may use cubic b-splines

to approximate the background intensities and piecewise constant functions to approximate the transfer functions (Hansen et al., 2015). Moreover, we allow m_0, m_1 to increase with the length of the observation window T . Write $\boldsymbol{\beta}_j = (\boldsymbol{\beta}_{j,0}, \boldsymbol{\beta}_{j,1}, \dots, \boldsymbol{\beta}_{j,p})^\top$. We define $\boldsymbol{\alpha}_j = (\boldsymbol{\alpha}^{(j,0)}, \boldsymbol{\alpha}^{(j,1)}, \dots, \boldsymbol{\alpha}^{(j,p)})^\top$ such that $\boldsymbol{\alpha}^{(j,0)} \in \mathbb{R}^{m_0}$ with

$$\alpha_l^{(j,0)} = \frac{1}{T} \int_0^T \phi_{0,l}(t) dN_j(t), \quad l = 1, \dots, m_0,$$

and $\boldsymbol{\alpha}^{(j,k)} \in \mathbb{R}^{m_1}$, $l = 1, \dots, p$ with

$$\alpha_l^{(j,k)} = \frac{1}{T} \int_0^T \int_0^t \phi_{1,l}(t-u) dN_k(u) dN_j(t), \quad l = 1, \dots, m_1.$$

Moreover, we define $\mathbf{G} \in \mathbb{R}^{(m_0+pm_1) \times (m_0+pm_1)}$ such that

$$\mathbf{G} = \begin{pmatrix} \mathbf{G}^{(0,0)} & \mathbf{G}^{(0,1)} & \dots & \mathbf{G}^{(0,p)} \\ \mathbf{G}^{(1,0)} & \mathbf{G}^{(1,1)} & \dots & \mathbf{G}^{(1,p)} \\ \vdots & \vdots & \ddots & \vdots \\ \mathbf{G}^{(p,0)} & \mathbf{G}^{(p,1)} & \dots & \mathbf{G}^{(p,p)} \end{pmatrix}, \quad (6)$$

where the component $\mathbf{G}^{(k_1, k_2)}$ is defined as

$$\mathbf{G}_{l_1 l_2}^{(k_1, k_2)} = \begin{cases} \frac{1}{T} \int_0^T \phi_{0, l_1}(t) \phi_{0, l_2}(t) dt, & \text{if } k_1 = 0, k_2 = 0, \\ \frac{1}{T} \int_0^T \phi_{0, l_1}(t) \left\{ \int_0^t \phi_{1, l_2}(t-u) dN_{k_2}(u) \right\} dt, & \text{if } k_1 = 0, k_2 \neq 0, \\ \frac{1}{T} \int_0^T \left\{ \int_0^t \phi_{1, l_1}(t-u) dN_{k_1}(u) \right\} \phi_{0, l_2}(t) dt, & \text{if } k_1 \neq 0, k_2 = 0, \\ \frac{1}{T} \int_0^T \left\{ \int_0^t \phi_{1, l_1}(t-u) dN_{k_1}(u) \right\} \left\{ \int_0^t \phi_{1, l_2}(t-u) dN_{k_2}(u) \right\} dt, & \text{if } k_1 \neq 0, k_2 \neq 0. \end{cases}$$

With the above expressions for $\boldsymbol{\beta}_j$, $\boldsymbol{\alpha}_j$ and \mathbf{G} , we define

$$\ell_j(\boldsymbol{\beta}_j) \triangleq -2\boldsymbol{\beta}_j^\top \boldsymbol{\alpha}_j + \boldsymbol{\beta}_j^\top \mathbf{G} \boldsymbol{\beta}_j. \quad (7)$$

Some straightforward algebra shows that the loss function in (5) can be written as $\sum_{j=1}^p \ell_j(\boldsymbol{\beta}_j)$. Note that both $\boldsymbol{\alpha}_j$ and \mathbf{G} are calculated based on the observed event locations and the pre-specified basis functions (i.e., $\phi_0(t)$ and $\phi_1(t)$). Therefore, to estimate the background intensities and transfer functions, we can directly optimize (7) with respect to $\boldsymbol{\beta}_j$. Since the loss function $\sum_{j=1}^p \ell_j(\boldsymbol{\beta}_j)$ can be decomposed into p separate convex loss functions, i.e., $\ell_1(\boldsymbol{\beta}_1), \dots, \ell_p(\boldsymbol{\beta}_p)$, we can optimize each loss function separately.

Next, we define $\mathcal{E}_j = \{k : \omega_{j,k} \neq 0, 1 \leq k \leq p\}$. To estimate \mathcal{E}_j , we have $\hat{\mathcal{E}}_j = \{k : \hat{\omega}_{j,k} \neq 0, 1 \leq k \leq p\}$, where $\hat{\omega}_{j,k}$'s are the estimated transfer functions. Estimating $\omega_{j,k}$'s from

(7) will result in a densely connected network, as $\hat{\omega}_{j,k}$ may not be exactly zero, even when process k has no effect on process j . Note that if $\omega_{j,k} = 0$, then all coefficients associated with $\omega_{j,k}$ are zero (i.e., $\beta_{j,k} = 0$). Thus, to encourage sparsity in the estimated network, we impose a group lasso penalty on β_j , in which the coefficients in $\beta_{j,k}$ are grouped together, $k = 1, \dots, p$. Specifically, we consider the following optimization problem

$$\min_{\beta_j \in \mathbb{R}^{m_0 + pm_1}} -2\beta_j^\top \alpha_j + \beta_j^\top \mathbf{G} \beta_j + \eta_j \sum_{k=1}^p (\beta_{j,k}^\top \mathbf{G}^{(k,k)} \beta_{j,k})^{1/2}. \quad (8)$$

The penalty term $\sum_{k=1}^p (\beta_{j,k}^\top \mathbf{G}^{(k,k)} \beta_{j,k})^{1/2}$ is an extension of the standardized group lasso penalty (Simon et al., 2013). This optimization problem in (8) is convex and can be efficiently solved using a block coordinate descent algorithm (Simon et al., 2013). The terms $\alpha_1, \dots, \alpha_p$, and \mathbf{G} can be computed using standard numerical integration methods and such calculations can be carried out before implementing the block coordinate descent algorithm.

The tuning parameter η_j in the penalized least squared loss function in (8) controls the sparsity of β_j , and in turn controls the sparsity of the estimated network. To select the tuning parameter, we consider an eBIC-type function (Chen and Chen, 2008). Let $\hat{\beta}_j(\eta_j)$ be the parameter estimated from (8) with the tuning parameter η_j . The eBIC-type function is defined as

$$\text{eBIC}(\eta_j) = 2\ell_j \left\{ \hat{\beta}_j(\eta_j) \right\} \cdot \kappa_j + m_1 |\mathcal{E}_j| \cdot \frac{\log(T)}{T} + v \cdot m_1 |\mathcal{E}_j| \cdot \frac{\log(m_0 + m_1 p)}{T} \quad (9)$$

where $\kappa_j = T/N_j((0, T])$ is a scaling parameter, $|\mathcal{E}_j|$ is the cardinality of \mathcal{E}_j , and $0 \leq v \leq 1$ is a constant. We use $v = 0.5$ in our empirical studies.

4 Theory

In this section, we first show the existence of a thinning process representation of the proposed nonlinear and nonstationary Hawkes process. We then establish concentration inequalities for the first and second order statistics of the proposed point process. These results are useful in the subsequent analysis of the estimated intensity functions. The concentration inequalities are also of independent interest, as they provide important theoretical tools for analyzing statistical methods (e.g., regression analysis) that are applied to the proposed processes. Next, we establish the non-asymptotic error bound of the intensity functions estimated using the proposed method and show that our method can consistently identify the true edges in the network. Lastly, we propose a test statistic for testing if the background

intensities are constant in time, and derive its asymptotic null distribution. All proofs are collected in the Supplementary Materials.

4.1 Concentration inequalities

Studying the theoretical properties of the proposed class of Hawkes processes is challenging as most existing techniques are not applicable. For example, many existing theoretical analyses rely on the cluster process representation of the Hawkes process (Hawkes and Oakes, 1974; Bacry et al., 2015; Hansen et al., 2015), which assumes the transfer functions to be nonnegative. In this case, the Hawkes process can be viewed as a sum of independent processes (or clusters), and theoretical properties of the Hawkes process, such as the concentration inequality of the first and second order statistics, can be investigated by studying the properties of the independent processes. When negative transfer functions are permitted, however, the cluster process representation is no longer applicable. To overcome this challenge, Brémaud and Massoulié (1996) employed a thinning process representation of the Hawkes process, which did not require the transfer functions to be nonnegative. With this representation and a coupling result from Dedecker and Prieur (2004), Chen et al. (2017) was able to bound the temporal dependence of the Hawkes process and obtained a concentration inequality for the second order statistics. Both Brémaud and Massoulié (1996) and Chen et al. (2017) require the stationarity condition of the process. Moreover, Chen et al. (2017) focused on a linear Hawkes process (i.e., $h(\cdot)$ is linear). Hence, the results and techniques in Brémaud and Massoulié (1996) and Chen et al. (2017) are not directly applicable to our setting. In what follows, we first show the existence of a thinning process representation of the proposed nonlinear and nonstationary Hawkes process in (1).

Let $\bar{\mathbf{N}} = (\bar{N}_j)_{j=1,\dots,p}$ be a p -variate homogeneous Poisson process with intensity λ_{\max} , where $\lambda_{\max} \geq \lambda_j(t)$ for any t and j . Let $\lambda_j^{(0)}(t) = 0$, $j = 1, \dots, p$, and $N_j^{(0)} = \emptyset$. Construct recursively $\boldsymbol{\lambda}^{(n)}(t) = (\lambda_1^{(n)}(t), \dots, \lambda_p^{(n)}(t))^\top$ and $\mathbf{N}^{(n)} = (N_j^{(n)})_{j=1,\dots,p}$ as follows:

$$\begin{aligned} \lambda_j^{(n+1)}(t) &= h \left\{ \nu_j(t) + \int_0^t \sum_{k=1}^p \omega_{j,k}(t-u) dN_k^{(n)}(u) \right\}, \\ dN_j^{(n+1)}(t) &= 1_{[r_j^{(n+1)}(t) \leq \lambda_j^{(n+1)}(t)/\lambda_{\max}]} d\bar{N}_j(t), \quad j = 1, \dots, p, \end{aligned} \tag{10}$$

where ν_j and $w_{j,k}$ are as defined in (1). Moreover, $r_j^{(n+1)}(t) \sim \text{Unif}(0, 1)$ and is independent across t and j . It follows from Lemma A2 that $\lambda_j^{(n)}(t)$ is the intensity function of the point process $N^{(n)}(t)$. Next, we show that the sequence $\{\mathbf{N}^{(n)}\}_{n=1}^\infty$ in (10) converges in distribution

to the Hawkes process \mathbf{N} with intensity function (1). To that end, we introduce the following regularity condition.

Assumption 2. *Assume that there exists $\lambda_{\max} > 0$ such that $\lambda_j(t) \leq \lambda_{\max}$ for any t and j and $\{\omega_{j,k}, 1 \leq j, k \leq p\}$ are θ_0 -Lipschitz functions, for some $\theta_0 \geq 0$, with bounded support.*

This condition assumes that the intensities are bounded above by a constant. It also assumes that the transfer functions $\omega_{j,k}$'s are Lipschitz and have bounded support. The bounded support assumption has been fairly commonly considered in the analysis of multivariate Hawkes process (Hansen et al., 2015; Chen et al., 2017). Next, we state our first main theorem.

Theorem 1. *Let $\boldsymbol{\lambda}(t)$ be as defined in (1) satisfying Assumptions 1-2. Let $\{\boldsymbol{\lambda}^{(n)}(t)\}_{n=1}^{\infty}$ and $\{\mathbf{N}^{(n)}\}_{n=1}^{\infty}$ be sequences as defined in (10). We have that*

- (i) $\boldsymbol{\lambda}^{(n)}(t)$ converges to $\boldsymbol{\lambda}(t)$ almost surely for any t ,
- (ii) $\{\mathbf{N}^{(n)}\}_{n=1}^{\infty}$ converges in distribution to \mathbf{N} with intensity (1).

Theorem 1 shows the existence of a thinning process representation of the proposed non-stationary Hawkes Process. This is a key result in our theoretical analysis. Combining this result and the coupling technique in Chen et al. (2017), we are able to establish concentration inequalities for the first and second order statistics of the proposed Hawkes process. To that end, we additionally require the following condition.

Assumption 3. *There exists $\rho_{\Omega} \in (0, 1)$ such that $\sum_{k=1}^p \Omega_{j,k} \leq \rho_{\Omega}$, $j = 1, \dots, p$.*

This assumption requires that Ω has bounded column sums, which prevents the intensity function from concentrating on any single process. Recall that \mathcal{H}_t denotes the history of \mathbf{N} up to time t . For \mathcal{H}_t -predictable functions $f_1(\cdot)$ and $f_2(\cdot)$, define

$$y_k = \frac{1}{T} \int_0^T f_1(t) dN_k(t),$$

$$y_{j,k} = \frac{1}{T} \int_0^T \int_0^T f_2(t-t') dN_k(t') dN_j(t).$$

Theorem 2. *Suppose that there exists $\lambda_{\max} > 0$ such that $\lambda_j(t) \leq \lambda_{\max}$ for any t and j . Let $f_1(t)$ be a bounded function. We have, for any $1 \leq k \leq p$,*

$$\mathbb{P}(|y_k - \mathbb{E}y_k| \geq c_1 T^{-2/5}) \leq c_2 \exp(-T^{1/5}), \quad (11)$$

where c_1 and c_2 are positive constants. Let $f_2(t)$ be a bounded function on a bounded support. Under Assumptions 1-3, we have, for $1 \leq j \leq k \leq p$,

$$\mathbb{P}(|y_{j,k} - \mathbb{E}y_{j,k}| \geq c'_1 T^{-2/5}) \leq c'_2 T \exp(-c'_3 T^{1/5}), \quad (12)$$

where c'_1 , c'_2 and c'_3 are positive constants.

The proof of Theorem 2 is provided in the Supplementary Materials. In the proof, we first define a coupling process of \mathbf{N} using results from Theorem 1. This coupling process is used to bound the temporal dependence of \mathbf{N} . We then use a Bernstein type inequality for weakly dependent sequences (Merlevède et al., 2011) to obtain the final results.

Quantities such as y_k and $y_{j,k}$ appear in many statistical problems such as regression analysis (Massart, 2000) and clustering analysis (Chen et al., 2017). Therefore, establishing concentration inequalities for y_k and $y_{j,k}$ are important in the theoretical analysis of such methods. In the next corollary, we give an example of the application of Theorem 2.

Corollary 1. *Consider the matrix \mathbf{G} defined in (6). Under Assumptions 1-3, we have*

$$\mathbb{P}\left(\bigcap_{i \neq j} [|\mathbf{G}_{ij} - \mathbb{E}(\mathbf{G}_{ij})| \leq c_6 T^{-2/5}]\right) \geq 1 - c_4 (p+1)^2 T \exp(-c_5 T^{1/5}),$$

where c_4 , c_5 and c_6 are positive constants.

The result in Corollary 1 is a direct consequence of Theorem 2, once we show that the entries in \mathbf{G} are first and second order statistics of the proposed Hawkes process. Corollary 1 will be later used in deriving the non-asymptotic error bound of the estimated intensity functions and establishing edge selection consistency.

4.2 Non-asymptotic error bound

Recall that $\mathcal{E}_j = \{k : \omega_{j,k} \neq 0, 1 \leq k \leq p\}$ and let $s = \max_j |\mathcal{E}_j|$. Define $\Delta = (\Delta_0, \Delta_1, \dots, \Delta_p) \in \mathbb{R}^{m_0 + pm_1}$, such that $\Delta_0 \in \mathbb{R}^{m_0}$, $\Delta_k \in \mathbb{R}^{m_1}$, $1 \leq k \leq p$, and $\Delta \neq \mathbf{0}$. Let $\Delta_{\mathcal{E}_j} = (\Delta_0, (\Delta_k)_{k \in \mathcal{E}_j})$. Furthermore, define $\Psi(t) = (\Psi_0(t), \Psi_1(t), \dots, \Psi_p(t))$ where $\Psi_0(t) = \phi_0(t)$ and $\Psi_k(t) = \int_0^t \phi_1(t-u) dN_k(u)$, $k = 1, \dots, p$. Before we establish the non-asymptotic error bound, we introduce several regularity conditions.

Assumption 4. *There exists a positive number ξ_1 such that*

$$\min \left\{ \frac{\{\Delta^\top \mathbb{E}(\mathbf{G}) \Delta\}^{\frac{1}{2}}}{\|\Delta_{\mathcal{E}_j}\|_2} : \sum_{k \notin \mathcal{E}_j} \|\Delta_k\|_2 \leq \sum_{k \in \mathcal{E}_j} \|\Delta_k\|_2, 1 \leq j \leq p \right\} \geq \sqrt{\xi_1}.$$

This assumption is a form of the restricted eigenvalue assumption under the group lasso setting (Lounici et al., 2011). For example, it is immediately satisfied if $\mathbb{E}(\mathbf{G})$ has a positive minimal eigenvalue.

Assumption 5. *There exist $\gamma_{\min}, \gamma_{\max} > 0$ such that for $k = 1, \dots, p$*

$$\gamma_{\min} \leq \sigma_{\min}(\mathbb{E}(\mathbf{G}^{(k,k)})) \leq \sigma_{\max}(\mathbb{E}(\mathbf{G}^{(k,k)})) \leq \gamma_{\max},$$

where $\sigma_{\min}(\cdot)$ and $\sigma_{\max}(\cdot)$ denote the minimal and maximal eigenvalues, respectively.

This condition ensures that the basis functions are non-degenerate, and is useful in the analysis of the standardized group lasso penalty.

Assumption 6. *For $j = 1, \dots, p$, there exist $\tilde{\boldsymbol{\beta}}_j = (\tilde{\boldsymbol{\beta}}_{j,0}, \tilde{\boldsymbol{\beta}}_{j,1}, \dots, \tilde{\boldsymbol{\beta}}_{j,p})^\top \in \mathbb{R}^{m_0+pm_1}$ and constant $d \geq 2$ such that*

$$\frac{1}{T} \int_0^T \left\{ \boldsymbol{\Psi}^\top(t) \tilde{\boldsymbol{\beta}}_j - \lambda_j(t) \right\}^2 dt \leq b_2(s+1)^2 T^{-\frac{4d}{2d+1}}.$$

Here $m_0, m_1 = \lfloor b_1 T^{2/(2d+1)} \rfloor$ for some constants b_1 and b_2 , where $\lfloor x \rfloor$ denotes the largest integer less than x , and $\tilde{\boldsymbol{\beta}}_{j,k} = \mathbf{0}$ for $k \notin \mathcal{E}_j$.

This assumption guarantees that the true intensity function can be well approximated by the basis functions. That is, residuals from the truncated basis approximation decreases at a polynomial rate of the number of basis functions. This property holds for certain basis functions such as the normalized b-spline basis in Huang et al. (2010).

Next we establish the non-asymptotic error bound of the estimated intensity functions. Let $\hat{\boldsymbol{\beta}}_j$ be the estimator obtained from (8), and write $\hat{\lambda}_j(t) = \boldsymbol{\Psi}^\top(t) \hat{\boldsymbol{\beta}}_j$, $j = 1, \dots, p$.

Theorem 3. *Consider a Hawkes process on $(0, T]$ with intensity as defined in (1) satisfying Assumptions 1-6. Given $m_0, m_1 = \lfloor b_1 T^{2/(2d+1)} \rfloor$ and $\eta_j = \{\xi_1 \lambda_{\max} \log(p)/T\}^{1/2}$, we have for $j = 1, \dots, p$,*

$$\frac{1}{T} \int_0^T \left\{ \hat{\lambda}_j(t) - \lambda_j(t) \right\}^2 dt \leq 32 \left\{ b_2(s+1)^2 T^{-\frac{4d}{2d+1}} + 9s \lambda_{\max} \frac{\log(p)}{T} \right\}, \quad (13)$$

holds with probability at least $1 - C_6 p^{-1} - C_4 p^2 T \exp(-C_5 T^{1/5})$, where C_4, C_5 , and C_6 are positive constants, and b_1, b_2 are as defined in Assumption 6.

Theorem 3 shows the error bound of the intensity functions estimated from minimizing the penalized least squares loss in (8). The error bound on the right hand side of (13) consists

of two terms. The first term comes from the error of approximating the background and transfer functions using basis functions; the second term comes from the statistical error in the sparse estimation. We can see that if, for example, $\log(p) = o(T)$ and $s = O(\log(p))$, the approximation error becomes negligible and the error bound is dominated by the statistical error. Moreover, it is seen from (13) that the dimension p is allowed to grow much faster than the length of the observation window T .

4.3 Network structure recovery

In this section, we establish the network structure recovery consistency. Specifically, we show that our proposed method can consistently identify the true edges in the network with probability tending to one. To this end, we first introduce two assumptions.

Assumption 7. For all $j = 1, \dots, p$, we assume that

$$\max_{k \notin \mathcal{E}_j} \left\| \left\{ \mathbb{E} \int_0^T \boldsymbol{\Psi}_k(t) \boldsymbol{\Psi}_{\mathcal{E}_j}^\top(t) dt \right\} \left\{ \mathbb{E} \int_0^T \boldsymbol{\Psi}_{\mathcal{E}_j}(t) \boldsymbol{\Psi}_{\mathcal{E}_j}^\top(t) dt \right\}^{-1} \hat{g}_{\mathcal{E}_j} \right\|_2 \leq \frac{\gamma_{\min}}{\sqrt{2}},$$

where $\boldsymbol{\Psi}_{\mathcal{E}_j}(t) \in \mathbb{R}^{m_1 \cdot |\mathcal{E}_j|}$ is the concatenation of vectors $\{\boldsymbol{\Psi}_k(t) : k \in \mathcal{E}_j\}$, $\hat{g}_{\mathcal{E}_j}$ is the first order derivation of the penalty term $\sum_{k=1}^p (\boldsymbol{\beta}_{j,k}^\top \mathbf{G}^{(k,k)} \boldsymbol{\beta}_{j,k})^{1/2}$ and γ_{\min} is defined in Assumption 5.

This is a form of the irrepresentability condition under our setting. The irrepresentability condition is almost necessary in establishing the selection consistency for lasso estimators (Zhao and Yu, 2006; Van De Geer et al., 2009). It can be further relaxed if the adaptive lasso (Zou, 2006) or the SCAD (Fan et al., 2004) penalty terms are considered. The next condition is a minimal signal condition.

Assumption 8. There exists $\beta_{\min} > 0$ such that $\|\tilde{\boldsymbol{\beta}}_{j,k}\|_2 \geq \beta_{\min}$ for $k \in \mathcal{E}_j$, where $\tilde{\boldsymbol{\beta}}_j$ is as defined in Assumption 6.

With these two new assumptions and Theorem 3, we can now state the edge selection consistency property of our estimator.

Theorem 4. Consider a Hawkes process on $(0, T]$ with intensity as defined in (1) satisfying Assumptions 1-8. Assume that $m_0, m_1 = \lfloor b_1 T^{2/(2d+1)} \rfloor$, $\eta_j = \{\xi_1 \lambda_{\max} \log(p)/T\}^{1/2}$, and that $s = O(\log(p))$ and $\log(p) = o(T^{1/5})$. Then we have, for $j = 1, \dots, p$,

$$\hat{\mathcal{E}}_j = \mathcal{E}_j,$$

with probability at least $1 - C_6 p^{-1} - C_4 p^2 T \exp(-C_5 T^{1/5})$, where C_4 , C_5 and C_6 are the same constants as in Theorem 3.

This result on the selection consistency has an important implication in practice, as it ensures that our method can correctly identify the true edges in the latent network. We note that the selection consistency was also established in Chen et al. (2017), under a linear and stationary Hawkes process setting. In comparison, our result is established under the more flexible nonlinear and nonstationary setting. More importantly, our result also significantly relaxes a restrictive condition in Chen et al. (2017). Specifically, Assumption 7 in Chen et al. (2017), after some simplification, would require that $p = O(1)$. However, in our setting, p is allowed to grow at a faster rate than T (i.e., $\log(p) = o(T^{1/5})$).

4.4 Test of background intensity

In this section, we consider the problem of testing if the background intensities of the proposed Hawkes process are constant in time. If the background intensities $\nu_j(t)$'s in (1) are constant, under Assumption 1, a stationary process whose intensity follows (1) exists (Brémaud and Massoulié, 1996). In this case, if we further consider a linear Hawkes process, our proposed model reduces to that in Chen et al. (2017). However, if the background intensities are not constant, then the corresponding multivariate Hawkes process is nonstationary.

In our model, the background intensity $\nu_j(t)$ for the j th process is represented as $\phi_0(t)\beta_{j,0}$. Let the first term in the basis $\phi_0(t)$, i.e., $\phi_{01}(t)$, be the constant term. Testing if $\nu_j(t)$ is constant in time can be formulated as testing the following hypotheses:

$$H_0 : \mathbf{A}\beta_{j,0} = \mathbf{0} \quad vs. \quad H_1 : \mathbf{A}\beta_{j,0} \neq \mathbf{0} \quad (14)$$

where $\mathbf{A} = \begin{bmatrix} 0 & \mathbf{0}_{m_0-1} \\ \mathbf{0}_{m_0-1}^\top & \mathbf{I}_{(m_0-1) \times (m_0-1)} \end{bmatrix} \in \mathbb{R}^{m_0 \times m_0}$, where \mathbf{I} denotes the identity matrix. Let the penalized loss function in (8) be written as

$$\tilde{\ell}_j(\beta_j) = T \times \left\{ -2\beta_j^\top \alpha_j + \beta_j^\top \mathbf{G}\beta_j + \eta_j \sum_{k=1}^p (\beta_{j,k}^\top \mathbf{G}^{(k,k)} \beta_{j,k})^{1/2} \right\}.$$

Note that $\beta_{j,0}$ does not appear in the penalty term, that is, the coefficients from the background intensity are not penalized. We next define the test statistic as

$$L_j = \frac{1}{2} \left\{ \min_{\beta_j: \mathbf{A}\beta_{j,0} = \mathbf{0}} \tilde{\ell}_j(\beta_j) - \min_{\beta_j} \tilde{\ell}_j(\beta_j) \right\}.$$

Let $\tilde{\boldsymbol{\beta}}_{\mathcal{E}_j} = (\tilde{\boldsymbol{\beta}}_{j,0}, (\tilde{\boldsymbol{\beta}}_{j,k})_{k \in \mathcal{E}_j})$ and $\mathbf{B} = \begin{bmatrix} \mathbf{b} & \mathbf{0}_{m_1|\mathcal{E}_j|} \\ \mathbf{0}_{m_0 \times m_1|\mathcal{E}_j|} & \mathbf{I}_{m_1|\mathcal{E}_j| \times m_1|\mathcal{E}_j|} \end{bmatrix} \in \mathbb{R}^{(1+m_1|\mathcal{E}_j|) \times (m_0+m_1|\mathcal{E}_j|)}$, where $\tilde{\boldsymbol{\beta}}_j$ is as defined in Assumption 6, and $\mathbf{b} = (1, 0, \dots, 0) \in \mathbb{R}^{m_0}$. We define

$$\mathbf{V}_j = \frac{1}{T} \int_0^T \mathbb{E} \left\{ \boldsymbol{\Psi}_{\mathcal{E}_j}(t) \boldsymbol{\Psi}_{\mathcal{E}_j}^\top(t) \right\} \bar{\lambda}_j(t) dt,$$

where $\bar{\lambda}_j(t) = \mathbb{E}\{dN_j(t)\}/dt$ and define

$$\mathbf{Q}(\tilde{\boldsymbol{\beta}}_{\mathcal{E}_j}) = -\mathbb{E} \left\{ \frac{2}{T} \int_0^T \boldsymbol{\Psi}_{\mathcal{E}_j}(t) \boldsymbol{\Psi}_{\mathcal{E}_j}^\top(t) dt \right\}.$$

The following theorem states the asymptotic null distribution of the test statistic.

Theorem 5. *Assume that all conditions in Theorem 4 are satisfied. Under H_0 , we have that*

$$L_j \xrightarrow{\mathcal{D}} \sum_{i=1}^{m_0-1} \lambda_{j,i} \chi_i^2.$$

Here χ_i^2 's are independent $\chi^2(1)$ and $\lambda_{j,i}$'s are the eigenvalues of $\mathbf{V}_j^{1/2} \boldsymbol{\Sigma}_j \mathbf{V}_j^{1/2}$, where $\boldsymbol{\Sigma}_j = \mathbf{Q}(\tilde{\boldsymbol{\beta}}_{\mathcal{E}_j})^{-1} - \mathbf{B}^\top \{\mathbf{B} \mathbf{Q}(\tilde{\boldsymbol{\beta}}_{\mathcal{E}_j}) \mathbf{B}^\top\}^{-1} \mathbf{B}^\top$.

Based on the result in Theorem 5, we would reject the null $H_0 : \mathbf{A} \boldsymbol{\beta}_{j,0} = \mathbf{0}$ if $L_j \geq z_{1-\alpha}$, where z_α is the α th quantile of $\sum_{i=1}^{m_0-1} \lambda_{j,i} \chi_i^2$. In practice, both \mathbf{V}_j and $\mathbf{Q}(\tilde{\boldsymbol{\beta}}_{\mathcal{E}_j})$ need to be estimated and we estimate them with

$$\hat{\mathbf{V}}_j = \frac{1}{T} \int_0^T \left(\boldsymbol{\Psi}_{\hat{\mathcal{E}}_j}(t) \boldsymbol{\Psi}_{\hat{\mathcal{E}}_j}^\top(t) \right) \hat{\lambda}_j(t) dt,$$

$$\hat{\mathbf{Q}}(\tilde{\boldsymbol{\beta}}_{\mathcal{E}_j}) = -\frac{2}{T} \int_0^T \boldsymbol{\Psi}_{\hat{\mathcal{E}}_j}(t) \boldsymbol{\Psi}_{\hat{\mathcal{E}}_j}^\top(t) dt.$$

In Section 5, we carry out simulation studies to evaluate the type-I error rate and power of the proposed test.

5 Simulation Studies

In this section, we carry out simulation studies to investigate the finite sample performance of our proposed method, and to compare with existing solutions. We consider three simulation settings. In Simulation 1, we simulate data from the proposed Hawkes process and investigate the estimation accuracy of our proposed method. In Simulation 2, we simulate data from the proposed Hawkes process and investigate the network construction accuracy. In Simulations

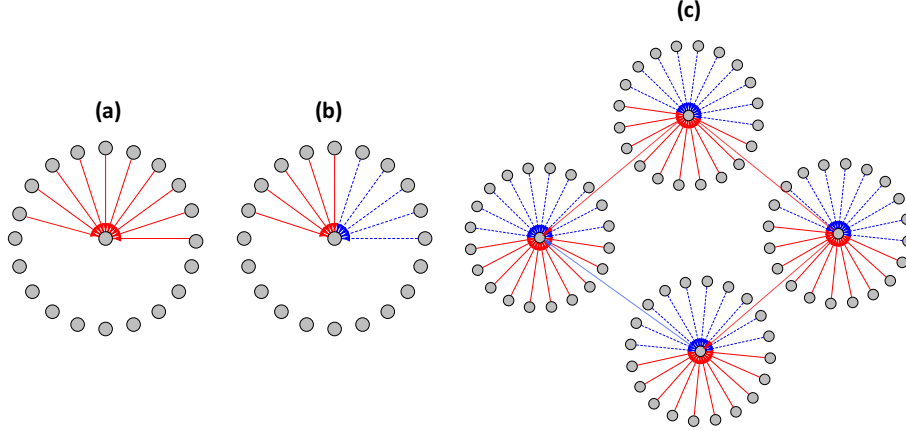


Figure 1: Directed network structures in simulation studies. The network in (a) is considered in Setting 1 of Simulation 1; the network in (b) is considered in Setting 2 of Simulation 1; the network in (c) is considered in Simulation 3. Red (solid) edges represent excitatory effects and blue (dashed) edges represent inhibitory effects.

1 and 2, we compare our method with [Chen et al. \(2017\)](#), which was proposed for linear Hawkes processes with constant background intensities. We also compare with a binning based approach in [Zhang et al. \(2016\)](#) on selection accuracy. Specifically, [Zhang et al. \(2016\)](#) considers a binning approach that divides the observation window into several bins and models the number of events in each bin. The network structure is then estimated using a regularized generalized linear model framework. In Simulation 3, we evaluate the type-I error rate and power of our proposed test of hypothesis. In all simulations, we use the criterion in (9) to select the tuning parameter for our method. The tuning parameters in [Chen et al. \(2017\)](#) and [Zhang et al. \(2016\)](#) are selected using their recommended BIC functions, respectively.

Simulation 1

In this simulation, we consider two different network settings. The first setting considers the network in Figure 1(a), where all transfer functions are positive, corresponding to excitatory effects. The second setting considers the network in Figure 1(b), where there are both positive and negative transfer functions, corresponding to excitatory and inhibitory effects, respectively. Let the network edge set be $\mathcal{E} = \{(k, 1), k = 2, \dots, 11\}$. The background intensity functions and transfer functions for each setting are as follows

- **Setting 1:**

$$\begin{aligned}\nu_j(t) &= \alpha_j + \alpha_j * \sin(2\pi t/T), \quad j = 2, \dots, 21 \\ \omega_{1,k} &= 20000(x + 0.001) \exp(1 - 500x), \quad k = 2, \dots, 11\end{aligned}$$

- **Setting 2:**

$$\begin{aligned}\nu_j(t) &= \alpha_j + \alpha_j * \sin(2\pi t/T), \quad j = 2, \dots, 21 \\ \omega_{1,k} &= 20000(x + 0.001) \exp(1 - 500x), \quad k = 2, \dots, 6 \\ \omega_{1,k} &= -10000(x + 0.001) \exp(1 - 500x), \quad k = 7, \dots, 11\end{aligned}$$

where α_j is generated from $N(30, 5^2)$ and $\nu_1(t) = 60 + 50 * \sin(2\pi t/T)$. We let the supports of all transfer functions be $[0, 0.01]$, and simulate events in $(0, T]$ with the intensity function (1) under Settings 1-2. To estimate the background intensities, we use cubic b-spline basis with one equally spaced internal knot in $[0, T]$. To estimate the transfer functions, we use cubic b-spline basis with three equally spaced internal knots in $[0, 0.01]$. We have also considered a larger range and/or more knots for the b-spline basis, and the results are very similar. We thus focus on the current setting when reporting our simulation results. To evaluate the estimation accuracy, we report the mean squared errors. For the background intensity, it is calculated as

$$\text{MSE}_j(\nu) = \left\{ \int (\hat{\nu}_j(t) - \nu_j(t))^2 dt \right\}^{1/2},$$

where $\hat{\nu}_j(t)$ is the estimate of $\nu_j(t)$. For the transfer functions, it is calculated as

$$\text{MSE}_j(\omega) = \left\{ \sum_{k=1}^p \int (\hat{\omega}_{j,k}(t) - \omega_{j,k}(t))^2 dt \right\}^{1/2},$$

where $\hat{\omega}_{j,k}(t)$ is the estimate of $\omega_{j,k}(t)$. To evaluate the selection accuracy, we report the F_1 score calculated as $2TP/(2TP+FP+FN)$, where TP is the true positive count, FP is the false positive count, and FN is the false negative count. For our proposed method and [Chen et al. \(2017\)](#), we report both the estimation and selection accuracy. For [Zhang et al. \(2016\)](#), we only report the selection accuracy, as their approach cannot estimate the intensity functions. [Table 1](#) reports the average criteria from the three methods, with the standard errors in the parentheses, over 100 data replications. Our proposed method is seen to achieve the best performance, both in terms of the estimation accuracy and selection accuracy, and this holds true for different observation window length T . Moreover, it is seen that the estimation error of our method decreases as T increases. Such an observation agrees with our theoretical result in [Theorem 3](#).

Setting 1		MSE ₁ (ν)	MSE ₁ (ω)	F ₁ score
$T = 10$	Proposed method	44.783 (2.501)	8.675 (0.115)	0.900 (0.007)
	Chen et al. (2017)	165.955 (1.072)	10.922(0.087)	0.646 (0.001)
	Zhang et al. (2016)	-	-	0.823 (0.006)
$T = 20$	Proposed method	37.641 (1.528)	5.585 (0.059)	0.961 (0.004)
	Chen et al. (2017)	232.408 (0.988)	7.855 (0.044)	0.654 (0.002)
	Zhang et al. (2016)	-	-	0.872 (0.006)
Setting 2		MSE ₁ (ν)	MSE ₁ (ω)	F ₁ score
$T = 10$	Proposed method	37.840 (2.176)	6.280 (0.079)	0.837 (0.008)
	Chen et al. (2017)	163.853 (0.796)	8.200 (0.059)	0.648 (0.001)
	Zhang et al. (2016)	-	-	0.574 (0.005)
$T = 20$	Proposed method	34.934 (1.668)	4.170 (0.048)	0.933 (0.006)
	Chen et al. (2017)	231.906 (0.665)	6.035 (0.029)	0.666 (0.002)
	Zhang et al. (2016)	-	-	0.560 (0.007)

Table 1: Comparison of the three methods with varying observation window length T . The standard errors are shown in the parentheses.

Simulation 2

In this simulation, we evaluate the graph construction accuracy of our proposed method. We consider an underlying directed network with $p = 84$ nodes that has multiple star-structured components, with both excitatory and inhibitory effects, as shown in Figure 1(c). For the four hub nodes (i.e., nodes with the most connections), the background intensity is set as $100 + 80\pi \sin(2\pi ft/T)$. For the rest of the nodes, the background intensity is set as $\alpha_j + \alpha_j\pi \sin(2\pi ft/T)$, where α_j is generated independently from $N(60, 5^2)$ for each node. This setting characterizes the varying background intensities among nodes in real applications. The transfer functions for excitatory and inhibitory connections are set as in Setting 2 of Simulation 1. We let the support of all transfer functions be $[0, 0.01]$, and simulate events in $(0, T]$ with the intensity function (1) with $f = 5$ and $T = 20$. To estimate the background intensities, we use cubic b-spline basis with sixteen equally spaced internal knots in $[0, T]$. To estimate the transfer functions, we use cubic b-spline basis with three equally spaced internal knots in $[0, 0.01]$. Table 2 compares the false negative rate, false positive rate and F₁ score of the three methods over 100 data replications. We can see the proposed method

	FNR	FPR	F ₁ score
Proposed method	0.085 (0.003)	0.002 (0.001)	0.888 (0.003)
Chen et al. (2017)	0.001 (0.001)	0.765 (0.001)	0.031 (0.001)
Zhang et al. (2016)	0.508 (0.002)	0.052 (0.001)	0.169 (0.001)

Table 2: Comparison of the false negative rate (FNR), false positive rate (FPR) and F₁ score in Simulation 2. The standard errors are shown in the parentheses.

achieves the largest F₁ score out of the three methods. In Table 2, [Chen et al. \(2017\)](#) shows a large false positive rate and this is likely due to the biased estimation of the background intensity functions; [Zhang et al. \(2016\)](#) shows a large false negative rate and this is likely due to the loss of information in the binning approach.

Simulation 3

In this section, we evaluate the type-I error rate and power of the proposed test for background intensities. To investigate the type-I error rate, we consider the following setting

- **Setting 3:**

$$\nu_j(t) = \alpha_j, \quad j = 2, \dots, 21,$$

$$\omega_{1,k} = 10000(x + 0.001) \exp(1 - 500x), \quad k = 2, \dots, 11,$$

where α_j is generated from $N(30, 5^2)$ and $\nu_1(t) = 60 + 50 * \sin(2\pi t/T)$. We let the supports of all transfer functions be $[0, 0.01]$, and simulate events in $(0, T]$ with $T = 20$. The b-spline bases for estimating the background intensities and transfer functions are set as in Simulation 1. Figure 2 shows type-I error rate under varying significance levels. It is seen that the proposed test has type-I errors that are close to the nominal levels. Next, to examine the power of the proposed test, we consider the following setting

- **Setting 4:**

$$\nu_j(t) = \alpha_j + \alpha_j * \sin(2\pi t/T), \quad j = 2, \dots, 21,$$

$$\omega_{1,k} = 10000(x + 0.001) \exp(1 - 500x), \quad k = 2, \dots, 11,$$

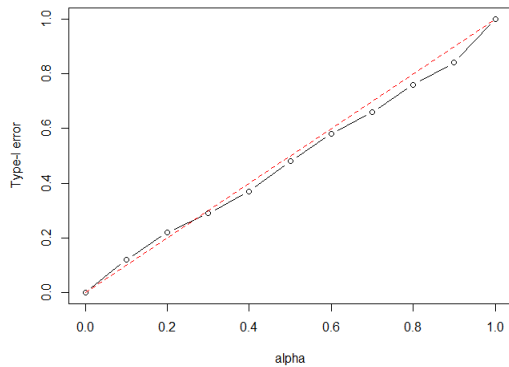


Figure 2: Type-I error rate under varying significance levels. The black solid line marks the estimated values and the red dashed line marks the theoretical values.

where α_j is generated from $N(30, 5)$ and $\nu_1(t) = 60 + 50 * \sin(2\pi t/T)$. We let the supports of all transfer functions be $[0, 0.01]$, and simulate events in $(0, T]$ with $T = 20$. The b-spline bases for estimating the background intensities and transfer functions are set as in Simulation 1. We perform the test of hypothesis based on 100 data replications. When the significant level is set to $\alpha = 0.05$, the proportion of rejection is 98%, which suggests that our proposed test is powerful against the alternatives.

6 Application to Neurophysiological Data

In this section, we apply our proposed method to a neuron spike train data set and estimate the functional connectivity network of neurons in the rat prefrontal cortex. The data were obtained from adult male Sprague-Dawley rats performing a T-maze based delayed-alternation task of working memory (Devilbiss and Waterhouse, 2004). In the experiment, the animal was trained to navigate down the T-maze and choose one of two arms (opposite to the one previously visited) for food rewards. In each trial, the animal was released after being placed in a start box for a fixed length of delay. On a correct trial (i.e., the arm with food was chosen), the animal was rewarded and returned to the start box. On an incorrect trial (i.e., the arm without food was chosen), the animal was returned to the start box without being rewarded. In the study, the animal remained in a training period until it reached 90%-100% accuracy on 40 trials. After the training period, a recording session was performed. The spike train recording consisted of 73 neurons in an experiment of 40 trials. Each trials took about 36 seconds and the total recording had 1434.22 seconds. See Zhang

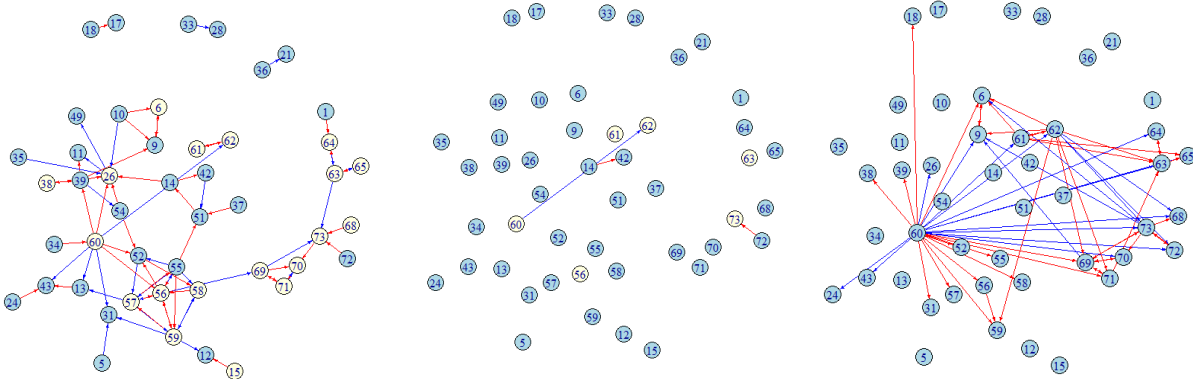


Figure 3: Estimated neuronal networks. Left: the proposed method; middle: [Chen et al. \(2017\)](#); right: [Zhang et al. \(2016\)](#). The red and blue arrows represent excitatory and inhibitory effects, respectively. Light colored nodes represent neurons that have self-exciting effects.

[et al. \(2016\)](#) for more information about data collection and processing.

We applied our proposed method to this dataset. To estimate the background intensity, we considered cubic b-splines with 20 equally spaced internal knots in the observation window. To estimate the transfer functions, we considered step function basis with 4 equally spaced knots in $[0, 2]$. We have also considered a larger range and/or more knots for the basis functions, and the results are very similar. The eBIC in (9) was used to select the tuning parameters. First, we performed the proposed test of hypothesis for each neuron to assess the if the background intensity is constant in time. Based on the p -values from the tests, 38 neurons had time-varying background intensity functions (significance level was set to 0.05). Next, we move to estimate the neuronal connectivity network. When estimating the network structure, we also considered [Chen et al. \(2017\)](#) and [Zhang et al. \(2016\)](#). The tuning parameters in [Chen et al. \(2017\)](#) and [Zhang et al. \(2016\)](#) were selected using their recommended BIC functions, respectively. Figure 3 shows the estimated neuronal networks from the three different methods. We can see all three estimated networks are sparse, with both excitatory and inhibitory relationships. However, their structures are quite different. The network estimated from our method is highly clustered and has a power-law degree distribution, which are two unique features of real world networks ([Barabási and Albert, 1999](#)). Also interestingly, about 70% of the identified edges in our estimated network are within the right prefrontal cortex, which agrees with existing findings that the right prefrontal cortex is highly related to the episodic memory retrieval ([Henson et al., 1999](#)). The biological

significance of the identified edges requires further investigation.

Compared to our estimated network, [Chen et al. \(2017\)](#) identified a very sparse network. This difference is likely due to the bias in estimating the background intensity function from their method. [Zhang et al. \(2016\)](#) also identified a very different network structure. This network has two hub (or densely connected) nodes, namely, neurons 60 and 62, and a small clustering coefficient. We find that neurons 60 and 62 are the two most frequently fired neurons in the ensemble. Specifically, neurons 60 and 62 have 14,433 and 8,191 firing events, respectively, while other neurons have on average 501 firing events during the experiment. The regularized generalized linear model framework in [Zhang et al. \(2016\)](#) penalizes the frequently and infrequently firing neurons equally when encouraging sparsity. This can potentially lead to over selection for the frequently firing neurons, and under selection for the infrequently firing neurons.

References

- Amari, S.-i. (1977), “Dynamics of pattern formation in lateral-inhibition type neural fields,” *Biological cybernetics*, 27, 77–87.
- Bacry, E., Delattre, S., Hoffmann, M., and Muzy, J.-F. (2013), “Modelling microstructure noise with mutually exciting point processes,” *Quantitative Finance*, 13, 65–77.
- Bacry, E., Gaïffas, S., and Muzy, J.-F. (2015), “A generalization error bound for sparse and low-rank multivariate Hawkes processes,” *arXiv preprint arXiv:1501.00725*.
- Barabási, A.-L. and Albert, R. (1999), “Emergence of scaling in random networks,” *science*, 286, 509–512.
- Brémaud, P. and Massoulié, L. (1996), “Stability of nonlinear Hawkes processes,” *The Annals of Probability*, 1563–1588.
- Chen, F. and Hall, P. (2013), “Inference for a nonstationary self-exciting point process with an application in ultra-high frequency financial data modeling,” *Journal of Applied Probability*, 50, 1006–1024.
- Chen, J. and Chen, Z. (2008), “Extended Bayesian information criteria for model selection with large model spaces,” *Biometrika*, 95, 759–771.

- Chen, S., Shojaie, A., Shea-Brown, E., and Witten, D. (2017), “The multivariate Hawkes process in high dimensions: Beyond mutual excitation,” *arXiv preprint arXiv:1707.04928*.
- Costa, M., Graham, C., Marsalle, L., and Tran, V. C. (2018), “Renewal in Hawkes processes with self-excitation and inhibition,” *arXiv preprint arXiv:1801.04645*.
- Dedecker, J. and Prieur, C. (2004), “Coupling for τ -dependent sequences and applications,” *Journal of Theoretical Probability*, 17, 861–885.
- Devilbiss, D. M. and Waterhouse, B. D. (2004), “The effects of tonic locus ceruleus output on sensory-evoked responses of ventral posterior medial thalamic and barrel field cortical neurons in the awake rat,” *Journal of Neuroscience*, 24, 10773–10785.
- Engle, R. F. and Russell, J. R. (1998), “Autoregressive conditional duration: a new model for irregularly spaced transaction data,” *Econometrica*, 1127–1162.
- Fan, J., Peng, H., et al. (2004), “Nonconcave penalized likelihood with a diverging number of parameters,” *The Annals of Statistics*, 32, 928–961.
- Farajtabar, M., Wang, Y., Rodriguez, M. G., Li, S., Zha, H., and Song, L. (2015), “Coevolve: A joint point process model for information diffusion and network co-evolution,” in *Advances in Neural Information Processing Systems*, pp. 1954–1962.
- Hansen, N. R., Reynaud-Bouret, P., Rivoirard, V., et al. (2015), “Lasso and probabilistic inequalities for multivariate point processes,” *Bernoulli*, 21, 83–143.
- Hawkes, A. G. (1971), “Spectra of some self-exciting and mutually exciting point processes,” *Biometrika*, 58, 83–90.
- Hawkes, A. G. and Oakes, D. (1974), “A cluster process representation of a self-exciting process,” *Journal of Applied Probability*, 11, 493–503.
- Henson, R., Shallice, T., and Dolan, R. J. (1999), “Right prefrontal cortex and episodic memory retrieval: a functional MRI test of the monitoring hypothesis,” *Brain*, 122, 1367–1381.
- Huang, J., Horowitz, J. L., and Wei, F. (2010), “Variable selection in nonparametric additive models,” *Annals of statistics*, 38, 2282.

- Lemonnier, R. and Vayatis, N. (2014), “Nonparametric markovian learning of triggering kernels for mutually exciting and mutually inhibiting multivariate hawkes processes,” in *Joint European Conference on Machine Learning and Knowledge Discovery in Databases*, Springer, pp. 161–176.
- Lewis, E. and Mohler, G. (2011), “A nonparametric EM algorithm for multiscale Hawkes processes,” *Journal of Nonparametric Statistics*, 1, 1–20.
- Linderman, S. and Adams, R. (2014), “Discovering latent network structure in point process data,” in *International Conference on Machine Learning*, pp. 1413–1421.
- Lounici, K., Pontil, M., Van De Geer, S., Tsybakov, A. B., et al. (2011), “Oracle inequalities and optimal inference under group sparsity,” *The Annals of Statistics*, 39, 2164–2204.
- Massart, P. (2000), “Some applications of concentration inequalities to statistics,” in *Annales de la Faculté des sciences de Toulouse: Mathématiques*, vol. 9, pp. 245–303.
- Merlevède, F., Peligrad, M., and Rio, E. (2011), “A Bernstein type inequality and moderate deviations for weakly dependent sequences,” *Probability Theory and Related Fields*, 151, 435–474.
- Ogata, Y. (1981), “On Lewis’ simulation method for point processes,” *IEEE Transactions on Information Theory*, 27, 23–31.
- Okatan, M., Wilson, M. A., and Brown, E. N. (2005), “Analyzing functional connectivity using a network likelihood model of ensemble neural spiking activity,” *Neural computation*, 17, 1927–1961.
- Roueff, F., Von Sachs, R., and Sansonnet, L. (2016), “Locally stationary Hawkes processes,” *Stochastic Processes and their Applications*, 126, 1710–1743.
- Simon, N., Friedman, J., Hastie, T., and Tibshirani, R. (2013), “A sparse-group lasso,” *Journal of Computational and Graphical Statistics*, 22, 231–245.
- Van De Geer, S. A., Bühlmann, P., et al. (2009), “On the conditions used to prove oracle results for the Lasso,” *Electronic Journal of Statistics*, 3, 1360–1392.
- Veen, A. and Schoenberg, F. P. (2008), “Estimation of space–time branching process models in seismology using an em–type algorithm,” *Journal of the American Statistical Association*, 103, 614–624.

- Vinci, G., Ventura, V., Smith, M. A., and Kass, R. E. (2016), “Separating spike count correlation from firing rate correlation,” *Neural computation*, 28, 849–881.
- Vinci, G., Ventura, V., Smith, M. A., Kass, R. E., et al. (2018), “Adjusted regularization in latent graphical models: Application to multiple-neuron spike count data,” *The Annals of Applied Statistics*, 12, 1068–1095.
- Wang, Y., Xie, B., Du, N., and Song, L. (2016), “Isotonic Hawkes processes,” in *International conference on machine learning*, pp. 2226–2234.
- Xu, H., Farajtabar, M., and Zha, H. (2016), “Learning granger causality for Hawkes processes,” in *International Conference on Machine Learning*, pp. 1717–1726.
- Zhang, C., Chai, Y., Guo, X., Gao, M., Devilbiss, D., and Zhang, Z. (2016), “Statistical Learning of Neuronal Functional Connectivity,” *Technometrics*, 58, 350–359.
- Zhao, P. and Yu, B. (2006), “On Model Selection Consistency of Lasso,” *Journal of Machine Learning Research*, 7, 2541–2563.
- Zhou, K., Zha, H., and Song, L. (2013), “Learning social infectivity in sparse low-rank networks using multi-dimensional Hawkes processes,” in *Artificial Intelligence and Statistics*, pp. 641–649.
- Zou, H. (2006), “The adaptive lasso and its oracle properties,” *Journal of the American statistical association*, 101, 1418–1429.